Celastrol downregulates E2F1 to induce growth inhibitory effects in hepatocellular carcinoma HepG2 cells

LIANG MA, LEI PENG, SHENG FANG, BANGGUO HE and ZI LIU

Department of Chemical Biology and Pharmaceutical Engineering, School of Chemistry and Chemical Engineering, Anhui University of Technology, Ma'anshan, Anhui 243002, P.R. China

Received March 7, 2017; Accepted August 9, 2017

DOI: 10.3892/or.2017.5971

Abstract. Celastrol, a natural compound extracted from *Tripterygium wilfordii*, is known to exhibit potential anticancer activities in various types of tumor cells. E2F1 is reported to be overexpressed in several types of human tumors and its inactivation may be a valuable novel potential therapeutic strategy for cancer treatment. However, the molecular mechanism underlying the pro-apoptotic effects of celastrol on hepatocellular carcinoma (HCC) cells remains unclear, and E2F1-targeted compounds have been rarely identified. In the present study, we demonstrated that celastrol inhibited the proliferation of human HCC cells and triggered apoptosis of HepG2 cells in a caspase-dependent manner. E2F1 was potently downregulated by celastrol in a dose- and time-dependent manner at both the mRNA and protein levels. Moreover, siRNA-mediated E2F1 silencing enhanced celastrol-induced apoptosis and inhibition of proliferation. Our data imply that downregulation of E2F1 may be a key factor in the celastrol-mediated inhibitory effects in HepG2 cells, and celastrol can serve as a leading compound for the development of compounds designed to inactivate E2F1 for HCC therapy.

Introduction

Hepatocellular carcinoma (HCC) is ranked as the fifth most common type of cancer worldwide and is considered as the third most common cause of cancer-related deaths (1). The first-line therapeutic protocol for HCC patients includes surgical treatment, such as liver resection and liver transplantation, but only for early-stage patients. Unfortunately, most HCC patients are often diagnosed at a late stage at which chemotherapy presents a unique advantage in the treatment for these patients (2). Due to the development of drug resistance in the treatment of HCC, it is necessary to develop novel chemotherapy drugs for the treatment of HCC.

The molecular mechanism underlying the development of HCC may be the disruption of a number of genes that function in different regulatory pathways, producing several molecular variants of HCC (3). Deregulation of E2F1 transcriptional activity is observed in a variety of cancers, including HCC, suggestive of the vital role of E2F1 in HCC pathogenesis (4). E2F1 is a transcription factor that controls cell fate including apoptosis. A recent study (5) reported that the downregulation of the transcription factor E2F1 was a key event contributing to the efficient induction and execution of ER stress-mediated cell apoptosis, and indicated that disruption of endoplasmic reticulum (ER) stress homeostasis, coupled with E2F1 gene expression modulation, may represent a new valuable target for the development of novel therapeutic strategies against chemoresistant tumor malignancies. Therefore, compounds that both negatively regulate the expression of E2F1 and trigger an ER stress-mediated apoptotic process may exhibit potential antitumor activity on chemoresistant cancers, such as HCC.

Celastrol, a natural compound extracted from *Tripterygium wilfordii*, has demonstrated promising antitumor activities in various cancer including HCC (6). Nonetheless, the exact mechanisms of action of celastrol in HCC have not been fully elucidated. It was reported that celastrol induces apoptosis evoked by ER stress (7,8). However, the effect of celastrol on E2F1 expression has never been reported. In the present study, we aimed to investigate the action of celastrol in HCC, with an emphasis on E2F1 modulation.

Materials and methods

Chemicals and reagents. Celastrol was purchased from Pie & Pie Technologies (Shenzhen, China). Proteasome inhibitor MG132 was obtained from Calbiochem (San Diego, CA, USA), PS-341 was obtained from Millennium Pharmaceuticals (Cambridge, MA, USA) and epoxomycin was purchased from the Peptide Institute (Osaka, Japan). Z-VAD-FMK was obtained from Beyotime Institute of Biotechnology (Shanghai, China). 3-(4,5-Dimethylthiazol-2-yl)-2,5-diphenyltetrazolium bromide (MTT) was purchased from Amresco (Solon, OH, USA). A stock solution of celastrol was prepared at 50 mM in

Correspondence to: Dr Zi Liu, Department of Chemical Biology and Pharmaceutical Engineering, School of Chemistry and Chemical Engineering, Anhui University of Technology, 59 Hudong Road, Ma'anshan, Anhui 243002, P.R. China
E-mail: tarring126@126.com

Key words: celastrol, E2F1, hepatocellular carcinoma, caspase, apoptosis

dimethyl sulfoxide (DMSO) and stored at -20˚C. The following antibodies were used: PARP, caspase-9 and cleaved caspase-3 (Cell Signaling Technology, Beverly, MA, USA), E2F1 (Santa Cruz Biotechnology, Santa Cruz, CA, USA) and actin (Sigma, St. Louis, MO, USA).

Cell culture. The HCC cell lines HepG2 and BEL-7402 were obtained from the Cell Bank of the Chinese Academy of Sciences (Shanghai, China). The lung adenocarcinoma cell line A549, large cell lung cancer line NCI-H460 and the breast cancer cell line MDA-MB231 were obtained from the American Tissue Culture Collection (ATCC; Manassas, VA, USA). Cells were maintained in Dulbecco's modified Eagle's medium (DMEM) supplemented with 10% fetal bovine serum (FBS) in a humidified incubator under 5% CO_2 at 37˚C as previously described (9).

Cell morphology. HepG2 cells were grown in culture flasks to 80-90% confluency. Then, the cells were treated with the indicated concentrations of celastrol for 18 h. Morphological changes in the cells were observed using an inverted microscope and photographed.

Cell viability. Cells were treated with celastrol at the indicated concentrations and time points. Cell viability was estimated by MTT assay, as previously described (10). Cells were cultured into a 96-well plate ($1x10^4$/well), and incubated with the indicated concentrations of celastrol (solvent of DMSO as the control group) when the cells were 80-90% confluent. After 44 h of treatment with celastol, 10 μl stock MTT solution was added to the culture medium (0.5 mg/ml final concentration) for incubation for an additional 4 h. Then, the medium was removed, and 150 μl DMSO was added to dissolve the solid formazan. The absorbance of each well was read at 490 nm using a microplate reader (Thermo Fisher Scientific, Inc., Waltham, MA, USA). The cell viability was calculated as a percent ratio of the absorbance of the sample cells to the absorbance of the control cells. Log (inhibitor) vs. response non-linear fit was used to estimate the IC_{50} value (GraphPad Prism 6.0; GraphPad Software, Inc., La Jolla, CA, USA).

Apoptosis assay. Cell apoptosis was detected using the Annexin V apoptosis detection kit (BD Biosciences, San Jose, CA, USA) according to the manufacturer's instructions. Briefly, cells were treated with celastrol at the indicated concentrations for 18 h, trypsinized and washed twice with cold phosphate-buffered saline (PBS). Then, the washed cell pellet was resuspended in 1.0 ml binding buffer at a concentration of 10^6 cells/ml and stained with 10 μl of Annexin V along with 20 μl 7-AAD for 15 min on ice in the dark. The samples were analyzed by flow cytometry (BD FACSCallbur) within 1 h.

RNA preparation and RT-PCR. Total RNA was extracted using the TRIzol reagent (Invitrogen, Carlsbad, CA, USA) and the phenol-chloroform extraction method according to the manufacturer's protocol. Total RNA (2 μg) was annealed with Oligo(dT) primers at 65˚C for 5 min. The cDNA was synthesized using a First Strand cDNA Synthesis kit (Fermentas, Hanover, MD, USA). Primers for E2F1 detection were as follows: sense primer, 5'-ACCAGGGTTTCCAGAGATGC-3' and antisense primer: 5'-CACCACACAGACTCCTTCCC-3' (11). The reaction mix contained: 2.5 μl 10X Ex Taq buffer, 2 μl dNTP mixture, 200 nM forward and reverse primers, 100 ng cDNA template, 0.25 μl Takara Ex Taq and ddH_2O up to 25 μl volume. The PCR cycling conditions consisted of the following: 98˚C for 10 sec for denaturation, 57˚C for 30 sec for annealing and 72˚C for 30 sec for extension, for a total of 30 cycles. Products of RT-PCR were separated by 1.5% agarose gel electrophoresis and detected using a gel imaging system.

siRNA assays and cell transfection. E2F1-specific RNA was designed and synthesized by Shanghai GenePharma Co. (Shanghai, China). Using Lipofectamine 2000 (Invitrogen; Thermo Fisher Scientific, Inc.) according to the manufacturer's protocol, HepG2 cells were transfected with 100 nM double-stranded siRNA oligonucleotides. After 48 h transfection, cells were treated with celastrol for additional 18 h, followed by western blotting and MTT assay, as previously decribed (12). The siRNA sequences of E2F1 were as follows: 5'-GAGGAGUUCAUCAGCCUUU-3'.

Western blot analysis. Cells were lysed in radioimmunoprecipitation assay lysis buffer [50 mM Tris-HCl pH 7.4, 150 mM NaCl, 0.1% sodium dodecyl sulfate (SDS), 1% Triton X-100, 1% deoxycholate, 1 mM ethylenediaminetetraacetic acid, 1 mM phenylmethanesulfonyl fluoride, 1 mM NaF, 1 mM sodium vanadate and protease inhibitors cocktail (Sigma)] and cleared by centrifugation to obtain whole-cell lysates. Then, equal amounts of proteins were subjected to SDS-polyacrylamide gel electrophoresis, and transferred to nitrocellulose membranes (Pall Corporation, Ann Arbor, MI, USA). After blocking with 5% skim milk, the membranes were incubated with primary antibodies at 4˚C overnight, and the membrane-bound antibodies were visualized using goat anti-rabbit or anti-mouse horseradish peroxidase-conjugated secondary antibodies (1:5,000 dilution; 1-2 h) and a chemiluminescent substrate (Thermo Fisher Scientific, Rockford, IL, USA). Equal loading of protein was confirmed by measuring total actin. The quantification of protein was analyzed using ImageJ software (National Institutes of Health, Bethesda, MD, USA). The dilution rates of primary antibodies used were: PARP, caspase-9 and cleaved caspase-3 (1:1,000); E2F1 (1:500); actin (1:100,00).

Statistical analysis. All experiments were repeated at least three times and the data are presented as the mean ± standard deviation unless noted otherwise. Differences between data groups were evaluated for significance using the Student's t-test of unpaired data by SPSS version 17.0 for Windows (SPSS, Inc., Chicago, IL, USA). $P<0.05$ was considered to indicate a statistically significant difference.

Results

Celastrol inhibits the growth of HCC cells. To evaluate the effect of celastrol on the growth of HCC cells, the MTT assay was used. HepG2 and Bel-7402 cells were treated with the indicated concentrations (0.5, 1, 2.5 and 5 μM) of celastrol (Fig. 1A) for 24 and 48 h. The assay results showed that

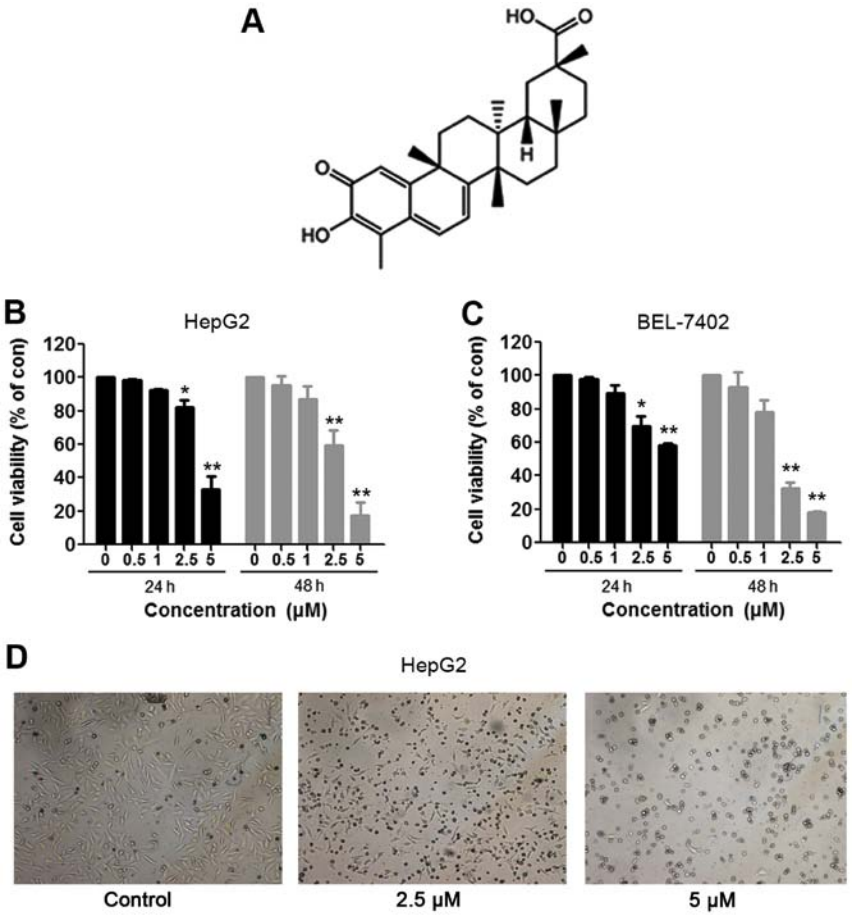

Figure 1. Celastrol inhibits the viability of HCC cells in a dose- and time-dependent manner. (A) Chemical structure of celastrol. (B) HepG2 cells were cultured in the presence of the indicated concentrations of celastrol for 24 and 48 h. The MTT assay was used to determine cell viability. The data are presented as the mean ± SD of three independent experiments, *P<0.05 and **P<0.01, compared with the control group. (C) Viability analysis of BEL-7402 cells incubated with the indicated concentrations of celastrol for 24 and 48 h, as evaluated by MTT assay. Data are expressed as mean ± SD, n=3, *P<0.05 and **P<0.01, compared with the control group. (D) The morphological changes in the HepG2 cells treated with the indicated concentrations of celastrol were observed via microscopy (magnification, x40). Representative images from three independent experiments are shown.

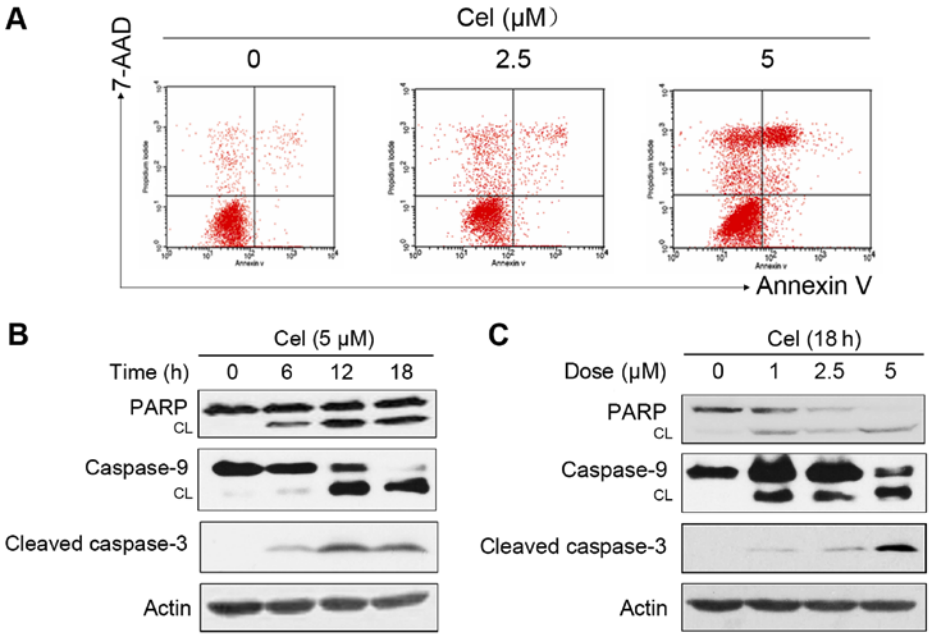

Figure 2. Celastrol induces apoptosis in HepG2 cells. (A) HepG2 cells were treated with the indicated doses of celastrol for 24 h. The cells were analyzed via flow cytometry after staining with Annexin V/7-AAD. HepG2 cells were incubated with 5 μM celastrol for the indicated time points (B) or treated with different concentrations of celastrol for 18 h (C). PARP, caspase-9 and cleaved caspase-3 were detected by western blotting. Cel, celastrol; CL, cleaved; PARP, poly(ADP ribose) polymerase.

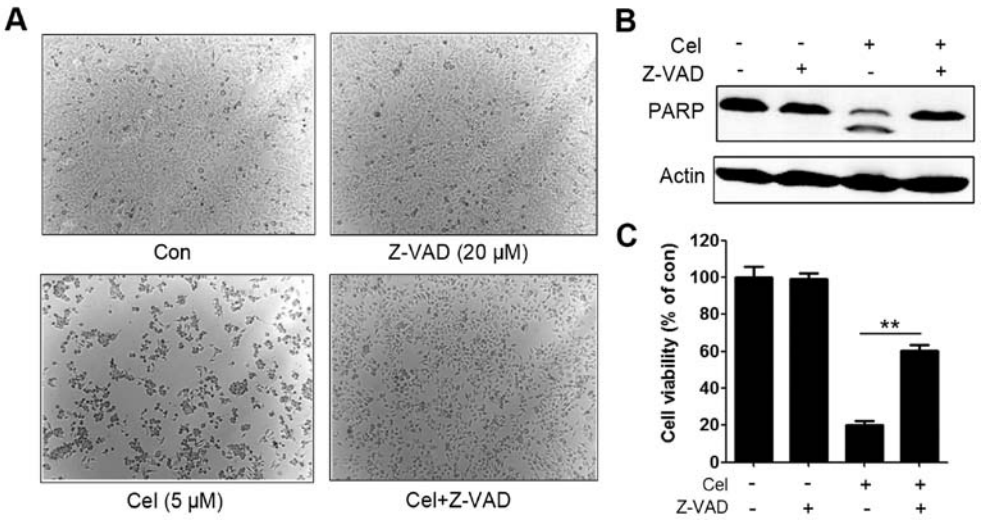

Figure 3. Caspase activation is involved in celastrol-induced apoptosis. (A) Representative images of HepG2 cells pretreated with Z-VAD-FMK (20 μM) for 1 h, followed by treatment with celastrol at 5 μM for 18 h; original magnification, x40. (B) HepG2 cells were pretreated with Z-VAD-FMK (20 μM) for 1 h, followed by treatment with celastrol at 5 μM for 18 h and lysed, and the lysates were subjected to western blotting using the indicated antibodies. (C) HepG2 cells were pretreated with Z-VAD-FMK (20 μM) for 1 h, followed by treatment with celastrol at 5 μM for 18 h, and cell viability was analyzed by MTT assay, **P<0.01, celastrol-treated group vs. celastrol and Z-VAD combination group. Cel, celastrol; Z-VAD, N-benzyloxycarbonyl-Val-Ala-Asp-fluoromethylketone; PARP, poly(ADP ribose) polymerase.

compared to the control cells, HepG2 cells incubated for 24 h exhibited viabilities of 98.5, 92.5, 82.0 and 33.2%, respectively, and the HepG2 cells treated for 48 h presented viabilities of 95.6, 87.0, 59.4 and 17.4%, respectively (Fig. 1B). The IC_{50} values of HepG2 cells for 24 and 48 h of celastrol treatment were 4.016 and 2.766 μM, respectively. In addition, the similar inhibitory effect also occurred in the BEL-7402 cells. As shown in Fig. 1C, relative to the control cells, BEL-7402 cells treated for 24 h exhibited viabilities of 97.9, 89.7, 69.6 and 58.6%, respectively, and the BEL-7402 cells treated for 48 h presented viabilities of 92.9, 78.0, 32.4 and 18.1%, respectively. The IC_{50} values of BEL-7402 cells for 24 and 48 h treatment of celastrol were 6.079 and 1.856 μM, respectively. In addition, obvious morphological changes were observed following treatment of celastrol in the HepG2 cells (Fig. 1D). Our results indicated that celastrol inhibited the viability of the HCC cells in a dose- and time-dependent manner.

Celastrol induces apoptosis in HepG2 cells. We investigated whether the cytotoxic effect of celastrol was associated with apoptosis in the HepG2 cells. Annexin V/7-AAD-staining and flow cytometric assay showed that treatment of the HepG2 cells with celastrol for 24 h caused apoptosis in a proportion of the cells (Fig. 2A). To further dissect the molecular mechanism underlying celastrol-induced apoptosis, the effects of celastrol on caspase activation which is a pivotal step in apoptosis were examined. Western blotting revealed that incubation with increasing concentrations of celastrol led to a significant cleavage of caspase-9 and -3 in a dose- and time-dependent manner (Fig. 2B and C). We then followed the status of nuclear enzyme poly(ADP-ribose) polymerase (PARP) that is one of the main cleavage targets of caspase-3. PARP cleavage was enhanced in the celastrol-treated HepG2 cells in a dose- and time-dependent manner (Fig. 2B and C), which is commonly regarded as an apoptotic marker (13). Collectively, these results showed that celastrol caused apoptosis and the activation of the caspase cascade in HepG2 cells.

Celastrol-induced apoptosis in HepG2 cells is caspase-dependent. To further confirm the activation of caspases as an essential step in the apoptotic pathway induced by celastrol, a caspase inhibitor benzyloxycarbony (Cbz)-l-Val-Ala-Asp (OMe)-fluoromethylketone (Z-VAD-FMK) was administered. HepG2 cells were pretreated with 20 μM Z-VAD-FMK for 1 h, and then incubated with 5 μM celastrol for an additional 18 h. Morphological results showed that Z-VAD-FMK partially rescued celastrol-induced cell death (Fig. 3A). Western blotting further revealed that celastrol-triggered PARP cleavage was suppressed by Z-VAD-FMK (Fig. 3B). Z-VAD-FMK also partly inhibited celastrol-induced cell cytotoxicity in the HepG2 cells (Fig. 3C). These data suggested that celastrol induced apoptosis of the HepG2 cells in a caspase-dependent fashion.

Celastrol downregulates E2F1 expression. E2F1 is reported to be overexpressed in several types of human tumors (14) and its inactivation may be a valuable novel potential therapeutic strategy for cancer treatment (5). This concept prompted us to detect the effect of celastrol on E2F1 expression. Western blot analysis was performed after the cells were exposed to different concentrations of celastrol for 18 h. As shown in Fig. 4A, the expression of E2F1 protein was reduced in the HepG2 cells exposed to celastrol at 1 μM and was apparently decreased in the cells treated with celastrol at 2.5 and 5 μM for 18 h. We further showed that celastrol caused E2F1 downregulation in a time-dependent manner (Fig. 4B). Apart from HCC cells, celastrol triggered a decrease in E2F1 in A549 and NCI-H460 lung cancer cells (Fig. 4C and D) and MDA-MB231 breast cancer cells (Fig. 4E and F). It has been reported that the proliferation factor c-Myc, as an important downstream target

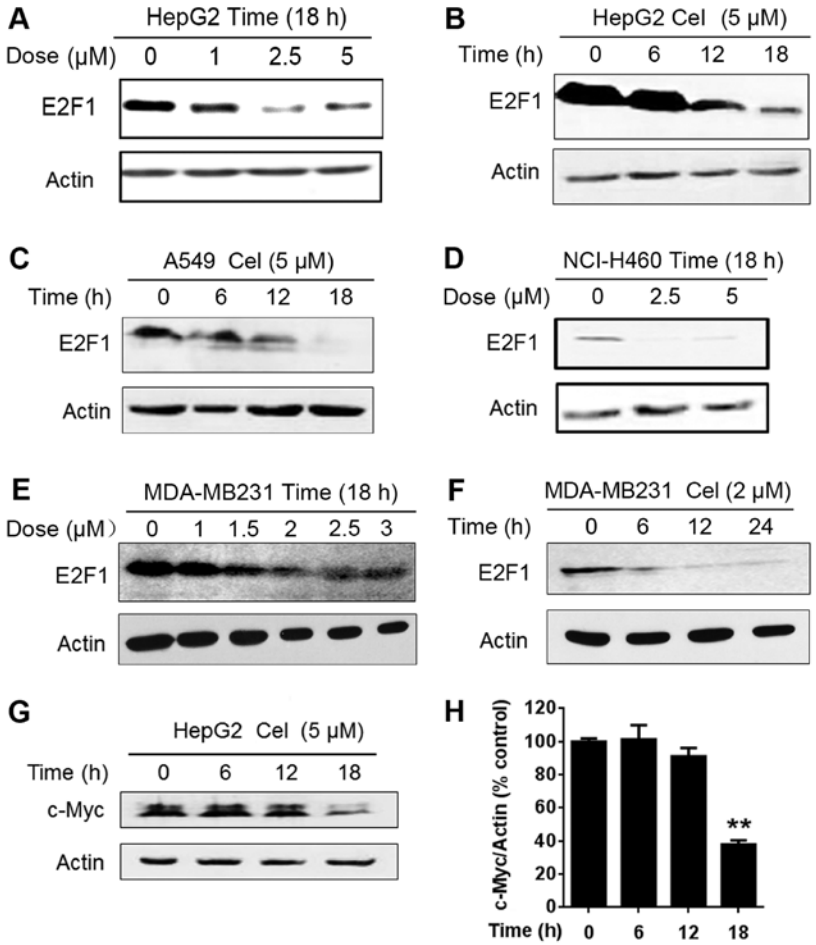

Figure 4. Downregualtion of E2F1 by celastrol. (A) HepG2 cells were incubated with the indicated concentrations of celastrol for 18 h, and cells were harvested for western blotting. (B) HepG2 cells were treated with celastrol (5 μM) for the indicated time points, and protein samples were obtained for western blot assay. A decrease in E2F1 protein was observed in lung cancer A549 (C), NCI-H460 (D) and breast cancer MDA-MB231 cells (E and F) via western blotting. (G) HepG2 cells were treated with celastrol (5 μM) for the indicated time points, and protein samples were subjected to western blot assay using c-Myc and actin antibodies. (H) Quantitative analysis of c-Myc protein expression from three independent experiments; **P<0.01 compared with the control group. Cel, celastrol.

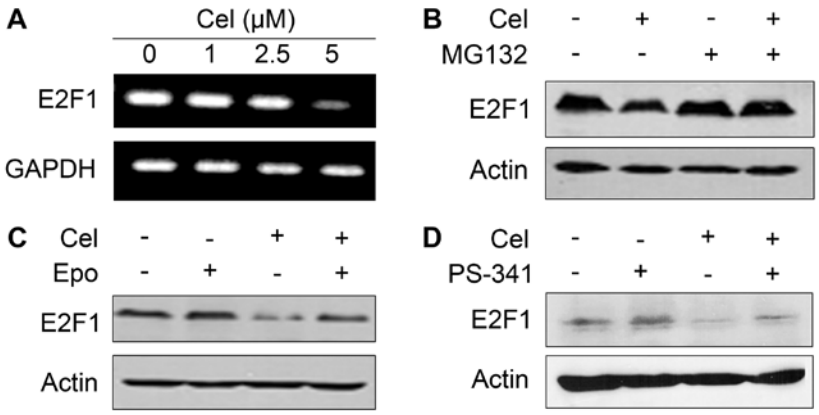

Figure 5. Celastrol triggers a decrease in E2F1 both at the transcription and protein levels. (A) Reverse transcription-polymerase chain reaction assays of HepG2 cells upon treatment with celastrol at the indicated concentrations for 18 h. GAPDH was used as an internal reference. Western blot analysis of E2F1 expression in HepG2 cells pre-incubated with (B) 10 μM MG132, (C) 100 nM EPO and (D) 100 nM PS-341 for 2 h followed by treatment with celastrol (5 μM) for an additional 18 h. Cel, celastrol; EPO, epoxomycin.

of E2F1 (15,16), is amplified and an indicator of malignant potential and poor prognosis in HCC, suggestive of a vital role of c-Myc in HCC pathogenesis (17). Thus, we further detected the alteration of c-Myc. As shown in Fig. 4G and H, celastrol decreased c-Myc expression in a time-dependent manner. These results showed that celastrol induced time-dependent and dose-dependent downregulation of E2F1 protein, and the decrease was not cell type-specific.

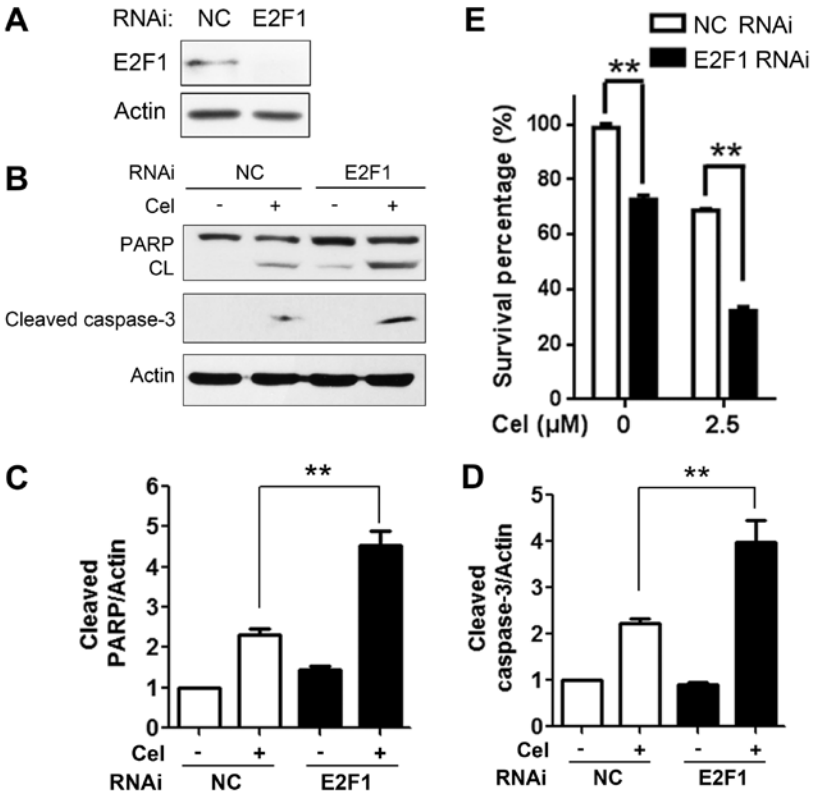

Figure 6. Celastrol-induced inhibitory effect is associated with downregulation of E2F1. (A) Reduced E2F1 expression by siRNA knockdown in HepG2 cells was detected by western blot analysis. (B) HepG2 cells were transfected with NC or E2F1-specific siRNA (100 nM) for 48 h, and then cultured for 18 h in the presence (2.5 μM) or absence of celastrol. Cell lysates were subjected to immunoblotting using the indicated antibodies. Quantitative analysis of (C) cleaved PARP and (D) cleaved caspase-3 protein levels from three independent experiments, which were adjusted to the actin protein level; **P<0.01. (E) HepG2 cells were transfected with NC or E2F1-specific siRNA (100 nM) for 48 h, followed by celastrol (2.5 μM) treatment for 18 h, and cell proliferation was assessed by MTT analysis. Cell viability of each group was normalized to the NC control group without treatment of celastrol. The mean ± SD of three independent experiments is shown; **P<0.01. NC, negative control; Cel, celastrol; PARP, poly(ADP ribose) polymerase; CL, cleaved; RNAi, RNA interference.

Celastrol decreases E2F1 at both the mRNA and protein levels. In order to investigate the mechanism underlying the downregulation of E2F1 protein, we firstly analyzed the expression of E2F1 at the mRNA level by RT-PCR assay. We found that E2F1 was reduced apparently in response to celastrol treatment at 5 μM for 18 h (Fig. 5A). Celastrol at 2.5 μM significantly suppressed E2F1 expression as detected by western blot assay (Fig. 4A), indicating that celastrol may also reduce E2F1 at the protein level. The ubiquitin-proteasome pathway is responsible for the degradation of most intracellular proteins in eukaryotic cells (18). We then tried to use classic proteasome inhibitors *in vitro* to examine the effect of these inhibitors on the degradation of E2F1 induced by celastrol. As shown in Fig. 5B-D, while proteasome inhibitor MG132, epoxomycin and PS-341 (19) did not influence E2F1 stability, pretreatment of HepG2 cells with these compounds markedly inhibited celastrol-triggered E2F1 degradation. These data indicated that celastrol downregulated E2F1 at both the mRNA and protein levels, and the decrease in E2F1 protein through a ubiquitin-proteasome pathway played a more important role in celastrol-induced E2F1 downregulation.

E2F1 downregulation is involved in the celastrol-induced inhibitory effect on HCC cells. E2F1-specific siRNA (Fig. 6A) was employed to evaluate its role in the celastrol-mediated inhibitory effects on HepG2 cells. Cells were transfected with siRNA targeting E2F1 for 48 h, followed by celastrol treatment for an additional 18 h, and apoptotic proteins were measured using western blot analysis. As presented in Fig. 6B-D, compared with the NC siRNA-treated cells, depletion of E2F1 resulted in potentiated cleavage of PARP and caspase-3 in the HepG2 cells upon celastrol treatment, suggestive of the enhancement of the apoptotic effect. In addition, cell proliferation was assessed by MTT assay. The result showed that knockdown of E2F1 alone partially inhibited the cell viability of HepG2 cells. Moreover, in responding to celastrol treatment, E2F1 depletion significantly enhanced celastrol-induced suppression of cell viability (Fig. 6E; n=3, P<0.01). These results indicated that E2F1 played an important role in the celastrol-induced antiproliferative and pro-apoptotic effects on HCC cells.

Discussion

Hepatocellular carcinoma (HCC) is the most common primary liver malignancy ranking fifth in incidence and third in mortality worldwide (1,20). Current therapies result in minimal survival advantage and are linked with drug resistance. Thus, a great challenge lies in identifying novel agents for HCC treatment. Natural compounds have been important sources of new drugs. Numerous successful anticancer drugs currently in use are derived from nature, and some of their analogues are under clinical trials (21). Celastrol, the main active ingredient of *Tripterygium wilfordii*, reveals a wide array of antitumor

activity against various types of cancers, containing HCC (22). In HCC C3A cells, celastrol was found to suppress growth and induce apoptosis through the modulation of STAT3/JAK2 signaling cascade *in vitro* and *in vivo* (6). In HCC Bel-7402 cells, celastrol triggered apoptosis via activation of the mitochondria-mediated pathway (23). Celastrol showed synergism combined with lapatinib in HCC HepG2 cells (24) and with ABT-737 in HepG2 and Bel-7402 cells (7). However, the molecular mechanism of action of celastrol in HCC therapy has not been well understood. The present study revealed for the first time that celastrol exerted its antiproliferative and pro-apoptotic effects partially mediated through modulation of E2F1 expression in HCC.

It is well known that inducing apoptosis in tumor cells is an important mechanism of action for many antitumor drugs. In the present study, antiproliferative evaluation showed that celastrol inhibited the growth of HCC HepG2 and Bel-7402 cells in a time- and dose-dependent manner. Flow cytometry revealed that apoptosis occurred in HepG2 cells after treatment of celastrol. The extrinsic and intrinsic apoptotic pathways are two common apoptotic pathways that lead to activation of initiator caspases (typically caspase-8 in the extrinsic pathway and caspase-9 in the intrinsic pathway) and ultimately effector caspases (caspase-3), which in turn cleaves downstream substrates, such as PARP (25,26). Accordingly, activation of apoptotic proteins indicative of cell apoptosis, including apparent cleavage of caspase-9 and -3, and PARP in a dose- and time-dependent way, was clearly observed by western blot analysis in HepG2 cells, suggesting that the intrinsic apoptotic pathway may be activated in celastrol-treated cells. In addition, we observed a rescue in celastrol-induced cell death in cells pretreated with a caspase inhibitor. These results indicate that caspase activation mediates celastrol-induced apoptosis.

The E2F1 transcription factor has been identified as a tumor-suppressor gene enhancing apoptosis by DNA damage in tumors lacking p53 (27). However, findings from transgenic models indicate that increased expression of E2F-1 occurs in c-myc/TGFα double transgenic mice during hepatocarcinogenesis and E2F-1 overexpression in the liver causes dysplasia and tumors (28). Moreover, abnormalities in E2F1 gene expression and/or E2F1 gene amplification have been described in various cancer cell lines and tumor types, including HCC (4,29,30). Notably, overexpression of E2F1 is frequently associated with high-grade tumors and poor patient survival prognosis (31). These data indicate that E2F1 has oncogenic functions in several types of cancer and may represent a rational therapeutic target. In the present study, we identified a natural compound celastrol that was capable of inducing a significant decrease in E2F1 in HCC HepG2 cells, as well as in lung cancer cells (A549 and NCI-H460) and breast cancer MDA-MB231 cells, implying that E2F1 suppression by celastrol is not a cell type-specific event, and celastrol could be a promising lead compound with potential anticancer activity in other E2F1-overexpressing human cancers, such as lung (32-34) and breast cancer (35). The proliferation factor c-Myc, an important downstream target of E2F1, was also decreased following celastrol treatment in a time-dependent manner, which may contribute to the observed antiproliferative effect of celastrol. Understanding of the mechanism by which E2F1 undergoes proteolytic breakdown is important to develop effective strategies for inactivation of E2F1 for HCC therapy. We demonstrated that celastrol not only downregulated E2F1 mRNA, but also reduced E2F1 protein via a ubiquitin-proteasome pathway. In addition, we first reported the role of E2F1 in the celastrol-mediated inhibitory effect as the siRNA assay revealed that depletion of E2F1 potentiated celastrol-mediated antiproliferative and pro-apoptotic activity in HepG2 cells. Pagliarini *et al* (5) reported that downregulation of E2F1 is required for ER-stress mediated apoptosis. ER stress was activated upon celastrol treatment in HCC cells (36), thus, the decrease in E2F1 may have been mediated by ER stress in celastrol-triggered apoptosis. This question warrants further investigation.

In conclusion, the present study provides initial evidence of an effect of E2F1 inhibition on the onset of celastrol-induced inhibitory activity in HCC cells, and celastrol may serve as a lead compound for the development of an E2F1 inhibitor.

Acknowledgements

The present study was supported by grants from the National Natural Science Foundation of China (nos. 81402511 and 81201577), and the Student Research Training Program of Anhui University of Technology (nos. 201510360171 and 2015024Z).

References

1. Attwa MH and El-Etreby SA: Guide for diagnosis and treatment of hepatocellular carcinoma. World J Hepatol 7: 1632-1651, 2015.
2. Llovet JM, Ricci S, Mazzaferro V, Hilgard P, Gane E, Blanc JF, de Oliveira AC, Santoro A, Raoul JL, Forner A, *et al*; SHARP Investigators Study Group: Sorafenib in advanced hepatocellular carcinoma. N Engl J Med 359: 378-390, 2008.
3. Thorgeirsson SS and Grisham JW: Molecular pathogenesis of human hepatocellular carcinoma. Nat Genet 31: 339-346, 2002.
4. Nakajima T, Yasui K, Zen K, Inagaki Y, Fujii H, Minami M, Tanaka S, Taniwaki M, Itoh Y, Arii S, *et al*: Activation of B-Myb by E2F1 in hepatocellular carcinoma. Hepatol Res 38: 886-895, 2008.
5. Pagliarini V, Giglio P, Bernardoni P, De Zio D, Fimia GM, Piacentini M and Corazzari M: Downregulation of E2F1 during ER stress is required to induce apoptosis. J Cell Sci 128: 1166-1179, 2015.
6. Rajendran P, Li F, Shanmugam MK, Kannaiyan R, Goh JN, Wong KF, Wang W, Khin E, Tergaonkar V, Kumar AP, *et al*: Celastrol suppresses growth and induces apoptosis of human hepatocellular carcinoma through the modulation of STAT3/JAK2 signaling cascade in vitro and in vivo. Cancer Prev Res 5: 631-643, 2012.
7. Feng L, Zhang D, Fan C, Ma C, Yang W, Meng Y, Wu W, Guan S, Jiang B, Yang M, *et al*: ER stress-mediated apoptosis induced by celastrol in cancer cells and important role of glycogen synthase kinase-3β in the signal network. Cell Death Dis 4: e715, 2013.
8. Fribley AM, Miller JR, Brownell AL, Garshott DM, Zeng Q, Reist TE, Narula N, Cai P, Xi Y, Callaghan MU, *et al*: Celastrol induces unfolded protein response-dependent cell death in head and neck cancer. Exp Cell Res 330: 412-422, 2015.
9. Ma L, Wen ZS, Liu Z, Hu Z, Ma J, Chen XQ, Liu YQ, Pu JX, Xiao WL, Sun HD, *et al*: Overexpression and small molecule-triggered downregulation of CIP2A in lung cancer. PLoS One 6: e20159, 2011.
10. Liu Z, Ma L, Wen ZS, Cheng YX and Zhou GB: Ethoxysanguinarine induces inhibitory effects and downregulates CIP2A in lung cancer cells. ACS Med Chem Lett 5: 113-118, 2013.
11. Liu JL, Zeng GZ, Liu XL, Liu YQ, Hu ZG, Liu Y, Tan NH and Zhou GB: Small compound bigelovin exerts inhibitory effects and triggers proteolysis of E2F1 in multiple myeloma cells. Cancer Sci 104: 1697-1704, 2013.

12. Liu Z, Ma L, Wen ZS, Hu Z, Wu FQ, Li W, Liu J and Zhou GB: Cancerous inhibitor of PP2A is targeted by natural compound celastrol for degradation in non-small-cell lung cancer. Carcinogenesis 35: 905-914, 2014.
13. Diefenbach J and Bürkle A: Introduction to poly(ADP-ribose) metabolism. Cell Mol Life Sci 62: 721-730, 2005.
14. Zhao Y, Tan J, Zhuang L, Jiang X, Liu ET and Yu Q: Inhibitors of histone deacetylases target the Rb-E2F1 pathway for apoptosis induction through activation of pro-apoptotic protein Bim. Proc Natl Acad Sci USA 102: 16090-16095, 2005.
15. Matsumura I, Tanaka H and Kanakura Y: E2F1 and c-Myc in cell growth and death. Cell Cycle 2: 333-338, 2003.
16. Lam SK, Li YY, Zheng CY, Leung LL and Ho JC: E2F1 down-regulation by arsenic trioxide in lung adenocarcinoma. Int J Oncol 45: 2033-2043, 2014.
17. Kawate S, Fukusato T, Ohwada S, Watanuki A and Morishita Y: Amplification of c-myc in hepatocellular carcinoma: Correlation with clinicopathologic features, proliferative activity and p53 overexpression. Oncology 57: 157-163, 1999.
18. Ciechanover A: Proteolysis: From the lysosome to ubiquitin and the proteasome. Nat Rev Mol Cell Biol 6: 79-87, 2005.
19. Adams J: The proteasome: A suitable antineoplastic target. Nat Rev Cancer 4: 349-360, 2004.
20. Huynh H: Molecularly targeted therapy in hepatocellular carcinoma. Biochem Pharmacol 80: 550-560, 2010.
21. Newman DJ and Giddings LA: Natural products as leads to antitumor drugs. Phytochem Rev 13: 123-137, 2014.
22. Liu Z, Ma L and Zhou GB: The main anticancer bullets of the Chinese medicinal herb, thunder god vine. Molecules 16: 5283-5297, 2011.
23. Li PP, He W, Yuan PF, Song SS, Lu JT and Wei W: Celastrol induces mitochondria-mediated apoptosis in hepatocellular carcinoma Bel-7402 cells. Am J Chin Med 43: 137-148, 2015.
24. Yan YY, Guo Y, Zhang W, Ma CG, Zhang YX, Wang C and Wang HX: Celastrol enhanced the anticancer effect of lapatinib in human hepatocellular carcinoma cells in vitro. J BUON 19: 412-418, 2014.
25. Nicholson DW: Caspase structure, proteolytic substrates, and function during apoptotic cell death. Cell Death Differ 6: 1028-1042, 1999.
26. Johnstone RW, Ruefli AA and Lowe SW: Apoptosis: A link between cancer genetics and chemotherapy. Cell 108: 153-164, 2002.
27. Engelmann D, Knoll S, Ewerth D, Steder M, Stoll A and Pützer BM: Functional interplay between E2F1 and chemotherapeutic drugs defines immediate E2F1 target genes crucial for cancer cell death. Cell Mol Life Sci 67: 931-948, 2010.
28. Conner EA, Lemmer ER, Omori M, Wirth PJ, Factor VM and Thorgeirsson SS: Dual functions of E2F-1 in a transgenic mouse model of liver carcinogenesis. Oncogene 19: 5054-5062, 2000.
29. Rabbani F, Richon VM, Orlow I, Lu ML, Drobnjak M, Dudas M, Charytonowicz E, Dalbagni G and Cordon-Cardo C: Prognostic significance of transcription factor E2F-1 in bladder cancer: Genotypic and phenotypic characterization. J Natl Cancer Inst 91: 874-881, 1999.
30. Zacharatos P, Kotsinas A, Evangelou K, Karakaidos P, Vassiliou LV, Rezaei N, Kyroudi A, Kittas C, Patsouris E, Papavassiliou AG, *et al*: Distinct expression patterns of the transcription factor E2F-1 in relation to tumour growth parameters in common human carcinomas. J Pathol 203: 744-753, 2004.
31. Engelmann D and Pützer BM: The dark side of E2F1: In transit beyond apoptosis. Cancer Res 72: 571-575, 2012.
32. Wu LC, Wen ZS, Qiu YT, Chen XQ, Chen HB, Wei MM, Liu Z, Jiang S and Zhou GB: Largazole arrests cell cycle at G1 phase and triggers proteasomal degradation of E2F1 in lung cancer cells. ACS Med Chem Lett 4: 921-926, 2013.
33. Gorgoulis VG, Zacharatos P, Mariatos G, Kotsinas A, Bouda M, Kletsas D, Asimacopoulos PJ, Agnantis N, Kittas C and Papavassiliou AG: Transcription factor E2F-1 acts as a growth-promoting factor and is associated with adverse prognosis in non-small cell lung carcinomas. J Pathol 198: 142-156, 2002.
34. Eymin B, Gazzeri S, Brambilla C and Brambilla E: Distinct pattern of E2F1 expression in human lung tumours: E2F1 is upregulated in small cell lung carcinoma. Oncogene 20: 1678-1687, 2001.
35. Han S, Park K, Bae BN, Kim KH, Kim HJ, Kim YD and Kim HY: E2F1 expression is related with the poor survival of lymph node-positive breast cancer patients treated with fluorouracil, doxorubicin and cyclophosphamide. Breast Cancer Res Treat 82: 11-16, 2003.
36. Zhu H, Yang W, He LJ, Ding WJ, Zheng L, Liao SD, Huang P, Lu W, He QJ and Yang B: Upregulating Noxa by ER stress, celastrol exerts synergistic anti-cancer activity in combination with ABT-737 in human hepatocellular carcinoma cells. PLoS One 7: e52333, 2012.